Seasonal influence of ENSO on the Atlantic ITCZ and equatorial South America

M. Münnich and J. D. Neelin

Department of Atmospheric and Oceanic Sciences, and Institute of Geophysics and Planetary Physics, University of California, Los Angeles, California, USA

Received 23 June 2005; revised 28 September 2005; accepted 5 October 2005; published 5 November 2005.

[1] In late boreal spring, especially May, a strong relationship exists in observations among precipitation anomalies over equatorial South America and the Atlantic intertropical convergence zone (ITCZ), and eastern equatorial Pacific and central equatorial Atlantic sea surface temperature anomalies (SSTA). A chain of correlations of equatorial Pacific SSTA, western equatorial Atlantic wind stress (WEA), equatorial Atlantic SSTA, sea surface height, and precipitation supports a causal chain in which El Niño/Southern Oscillation (ENSO) induces WEA stress anomalies, which in turn affect Atlantic equatorial ocean dynamics. These correlations show strong seasonality, apparently arising within the atmospheric links of the chain. This pathway and the influence of equatorial Atlantic SSTA on South American rainfall in May appear independent of that of the northern tropical Atlantic. Brazil's Nordeste is affected by the northern tropical Atlantic. The equatorial influence lies further to the north over the eastern Amazon and the Guiana Highlands.
Citation: Münnich, M., and J. D. Neelin (2005), Seasonal influence of ENSO on the Atlantic ITCZ and equatorial South America, *Geophys. Res. Lett.*, *32*, L21709, doi:10.1029/2005GL023900.

1. Introduction

[2] In interannual tropical Atlantic climate variability a few large-scale tropical sea surface temperature anomaly (SSTA) patterns are observed. One prominent pattern is a broad anomaly in the northern tropical Atlantic (NTA), north of the Atlantic's intertropical convergence zone (ITCZ). The cross-equatorial wind anomalies and related low-level moisture transport have been found to be important in precipitation anomalies over the Brazilian Nordeste region [*Hastenrath and Heller*, 1977; *Nobre and Shukla*, 1996]. EOF-based analyses often show a weaker, negative SSTA signal to the south [*Wang et al.*, 2004] which led to the notion of the "Atlantic dipole" [*Chang et al.*, 1997]. However, the statistical significance of this southern lobe is weak [*Enfield and Mayer*, 1997; *Sutton et al.*, 2000; *Dommenget and Latif*, 2000]. "Meridional mode" [*Ruiz-Barradas et al.*, 2003] or "gradient mode" [*Saravanan and Chang*, 2000; *Chiang et al.*, 2002] are now the preferred names for this pattern.

[3] A substantial portion the of the NTA variability has been attributed to El Niño Southern Oscillation (ENSO) [*Giannini et al.*, 2001; *Chang et al.*, 2000; *Enfield and Alfaro*, 1999]. ENSO leads to tropospheric warming throughout the Tropics. The heat capacity of the oceanic mixed layer leads to a delayed warming in the ocean, which is enhanced by reduced evaporation due to the reduce trade winds. A corresponding pattern in the southern tropical Atlantic has been analyzed by *Barreiro and Chang* [2002].

[4] Other SST patterns are linked to the tropical Atlantic upwelling region. These have been termed Atlantic Niño [*Merle*, 1980] or Bengulea Niño [*Florenchie et al.*, 2003], according to the region of SSTA, equatorial Atlantic or off Lower Guinea, respectively. The variability of these anomalies, however, are weaker in amplitude and shorter in period than El Niño [*Zebiak*, 1993]. Apparently, the atmospheric wind response to equatorial SSTA is too weak for the atmospheric wind feedbacks to play the same sustaining role as in ENSO, so Atlantic Niño events usually last only a few months. Recent studies [*Chiang et al.*, 2000] show decadal variability in the connection of ENSO and the equatorial Atlantic.

[5] Here we analyze the links among ENSO, equatorial Atlantic SSTA and precipitation, and show observational indications that Atlantic winds and equatorial ocean dynamics are involved.

2. Data Sets and Methods

[6] We analyze satellite based monthly data for precipitation (Climate Prediction Center Merged Analysis of Precipitation "CMAP" [*Xie and Arkin*, 1997]), SST (National Oceanic and Atmospheric Administration "OI.v2" [*Reynolds et al.*, 2002]) and sea level height (AVISO/altimetry data center "DT-MSLA" [*Ducet et al.*, 2000]) which start in 1979, 1982 and 1993, respectively. Analysis of longer SST records are based on the Met Office Hadley Centre's sea ice and sea surface temperature (SST) data set, "HadISST1.1". Satellite-based wind stress observations are too short, so for it we use reanalysis data (European Center for Medium-Range Weather Forecasts "ERA-40" [*Simmons and Gibson*, 2000]).

[7] When not mentioned otherwise, our analysis is based on 1/1982 to 9/2003. To get credible results for the limited time span we rely on rank correlation [*Hettmansperger and McKean*, 1998]. As a nonparametric statistical analysis technique, rank correlation provides significance levels without assuming Gaussianity of the observed fields.

3. Results

[8] Following *Zebiak* [1993], we select an Atl-3 index region 20°W–0°, 3°S–3°N which comprises the area of maximum SSTA variance in the equatorial region of the

0094-8276/05/2005GL023900$05.00

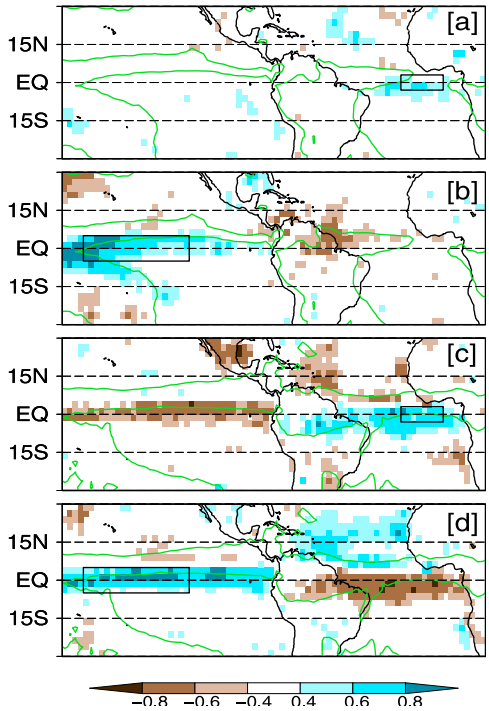

Figure 1. Comparison of rank correlation maps of SSTA indices with concurrent precipitation in (a, b) January and (c, d) May. The index regions (black rectangles) are (a, c) Atl-3 and (b, d) Niño-3.4. Green contours indicate 4 mm/day climatological precipitation.

Atlantic and define Atl-3 as the time series of mean SSTA in this region using the OI-V2 data. Monthly rank correlation (r_s) maps of precipitation with Atl-3 for the period 1982–2003 show significant correlation at the 95% level over the equatorial Atlantic ocean during all seasons. The precipitation anomalies tend to fall along the edge of the convergence zone, hinting at possible involvement of the upped ante mechanism [*Neelin et al.*, 2003; *Neelin and Su*, 2005]. Significant correlations are mostly confined to the equatorial ocean.

[9] In May the area of strong correlation is markedly larger than in other months, extending farther to the south and reaching deep into equatorial South America. The likely reason for this can be seen in Figure 1 which compares correlation maps of precipitation in January and May with ENSO (Niño-3.4 index, i.e., mean SSTA in the Niño-3.4 region, 170°W–120°W, 5°S–5°N) and the Atlantic Niño (Atl-3 index). In January (Figures 1a and 1b) the patterns are distinct, with ENSO having a drying effect over the Guiana region and out into the northern Tropical Atlantic while an Atlantic Niño is accompanied with increased rainfall along the equatorial Atlantic.

[10] In contrast, the May (Figures 1c and 1d) patterns are almost mirror images. Only the correlation with precipitation in the north-eastern Tropical Atlantic is absent for the Atlantic Niño. Indeed, the monthly r_s of Niño-3.4 with Atl-3 (Figure 2, circles) stays significant from April through August, peaking in May at 0.68 ($P > 99\%$) while it is insignificant during the rest of the year. Equatorial Atlantic/South American rainfall, ENSO and Atlantic equatorial SST are thus interconnected in late boreal spring. ENSO and the Atlantic Niño have been thought to vary independently [*Zebiak*, 1993; *Ruiz-Barradas et al.*, 2003]. However, *Latif and Barnett* [1995] found indications of a linkage of ENSO and Atlantic Niño for 1979 to 1988.

[11] Atlantic SSTA patterns associated with the Atlantic Niño and ENSO in May are depicted in Figure 3. For easier comparison, the ENSO pattern is plotted for the ENSO cold phase (La Niña). The linear regression map of negative Niño-3.4 with SSTA in the tropical Atlantic in May (Figure 3a) shows a pattern of positive regression coefficients along the equator and coastal upwelling region reminiscent of El Niño, with regressions coefficients peaking in the Atl-3 region. This equatorial pattern is weaker but otherwise similar to the regression map of Atl-3 with SSTA (Figure 3b) which exemplifies an Atlantic Niño. The wind stress patterns associated with Atl-3 and negative Niño-3.4 are southwesterly, peaking in the western equatorial Atlantic. In case of negative Niño-3.4, cooling wind anomalies reach further into the northern tropical Atlantic (NTA). They are accompanied by a weak cooling in the western half of the NTA region absent in the Atl-3 regression map. Note that the region of significant r_s of negative Niño-3.4 and Atl-3 wind speed (green contours) does not

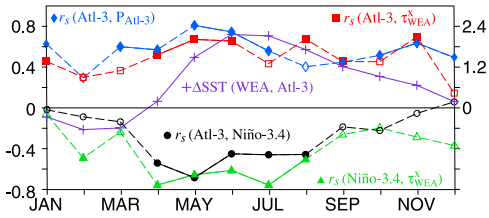

Figure 2. Monthly rank correlation of Atl-3 with (circles) Niño-3.4, (squares) zonal wind stress anomalies in the western equatorial Atlantic (WEA) and (diamonds) precipitation anomalies in the Atl-3 region and of Niño-3.4 with (triangles) zonal wind stress in WEA. Solid markers indicate correlations above the 95% significance level. Crosses give the climatological mean monthly temperature difference between SST in WEA and Atl-3 in C.

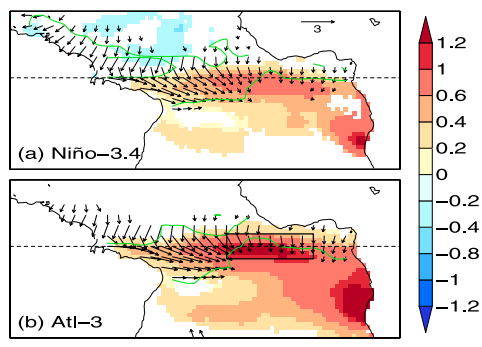

Figure 3. (a) Linear regression coefficient map of (color) SSTA and (arrows) wind stress anomalies (0.01 N/m^{2}C) versus negative Niño-3.4. For SSTA, only regions of at least 95% significant rank correlation are colored. For wind stress arrows the rank correlation for at least one of its zonal or meridional components is significant at the 95% level. (b) Same as (a) for Atl-3. The black rectangle marks the Atl-3 region.

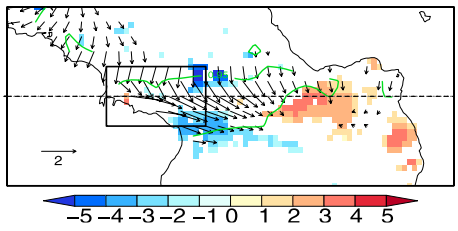

Figure 4. Linear regression coefficient map of (color) SSHA (m^3/N) and (arrows) wind stress anomalies (unitless) versus average zonal wind stress anomalies over the western Atlantic (50°W–30°W, 5°S–5°N, black rectangle). For SSHA, only regions of at least 95% significant rank correlation are colored. Wind stress arrows are drawn where rank correlation for at least one of its zonal or meridional components is significant at the 95% level. Green contour indicates the area of significant absolute wind stress rank correlation with the western Atlantic zonal wind stress.

correspond well with the SSTA pattern. Thus, while evaporative feedbacks may play a role, they do not appear to be the main cause of these SSTAs. The mechanism for the anomalies appears to be distinct from the NTA induced cross equatorial winds.

[12] Model studies [*Zebiak*, 1993; *Carton and Huang*, 1994; *Delecluse et al.*, 1994] have shown that, similar to ENSO, equatorial waves, excited by westerly wind anomalies in the western equatorial Atlantic lead to an Atlantic Niño. A map of rank correlation of sea-surface height anomalies (SSHA) averaged with zonal wind stress over WEA (30°W–50°W, 5°S–5°N) (Figure 4) confirms the remote connection between western equatorial wind stress and anomalies in the Atl-3 region. A positive SSHA, implying a deepened thermocline, peaks in the Atl-3 region with negative off-equatorial SSHA to the west, reminiscent of the observed equatorial Kelvin and Rossby wave packets that play a prominent role in ENSO. The May correlation of Atl-3 with SSHA reaches 0.89 in the Atl-3 region. Note that the positive SSHA lies to the east of the forcing wind anomalies (arrows). The r_s of Atl-3 with stress anomalies in WEA peaks when the wind stress anomalies lead Atl-3 by one month, supporting the interpretation that equatorial waves, excited in the west, are causing the Atlantic Niño.

[13] Furthermore, from April through August, the r_s of Niño-3.4 with WEA zonal stress anomalies (Figure 2, triangles) is higher than the r_s of Niño-3.4 with Atl-3 (Figure 2, circles). In general, wind is a noisier quantity than SST. One would thus expect correlations with it to be lower, so the higher correlation is another indicator that zonal wind stress anomalies are part of the causal chain from Nino-3.4 to equatorial Atlantic SSTA.

[14] How does the known NTA SSTA influence on Brazilian rainfall relate to the strong influence of equatorial SSTA? The time series of average SSTA in NTA (5°N–20°N, 15°W–80°W) and Atl-3 vary independently (r_s = 0.01) and Atl-3 does not show any significant correlation with SSTA in NTA (Figure 3b). Both influence May rainfall in the Nordeste region. The correlation patterns (Figures 1c and 5), however, are distinct. NTA SSTA influences precipitation over the eastern tip of South America whereas Atl-3 influence is more confined to the equatorial region but reaches deeper in to the Amazon basin (Figure 1c). Both together seem to add up to the influence of ENSO in May (Figure 1d).

[15] In recent decades the influence in spring of ENSO on the equatorial Atlantic has been strong [*Chiang et al.*, 2000]. A likely reason for this is shown in Figure 6 which illustrates the long-term change of Niño-3.4 standard deviation separately for each month of the year. Not only has ENSO been particularly strong in recent years, but ENSO variations strengthened during every month of the year. In fact the biggest percentage increase of ENSO variance occurred in October and May (Figure 6) while during the 1960s and 1970s ENSO was particularly weak in spring. It is thus likely that any existing correlation of ENSO and Atlantic Niño in that era, on which, e.g., the study of *Zebiak* [1993] was based, was hidden under background noise. The association with increased variance includes the impact of cold events and offers an alternative explanation to an SST threshhold postulated by *Chiang et al.* [2000].

4. Discussion

[16] Rank correlation analysis shows that precipitation anomalies over equatorial South America in May are linked with concurrent SST anomalies in the equatorial Atlantic and Pacific. While ENSO and the Atlantic Niño vary independently during ENSO's peak phase, they correlate well in late boreal spring and summer, for the satellite data period.

[17] Because this relationship was not seen in studies based on earlier periods, we first consider whether the two strong El Niños in this period might unduly impact the results. For the strongest El Niño, 1997/98, the following May Niño-3.4 is only the 6th largest overall. We also note that May Niño-3.4 SSTA correlates only at the 0.6 level

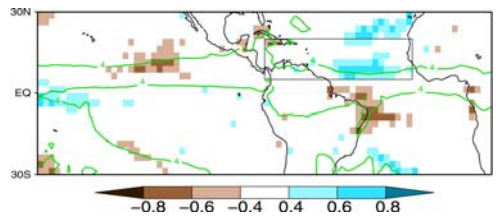

Figure 5. Rank correlation maps of average SSTA in NTA (black rectangle) with precipitation in May. Green contours indicate 4 mm/day climatological precipitation.

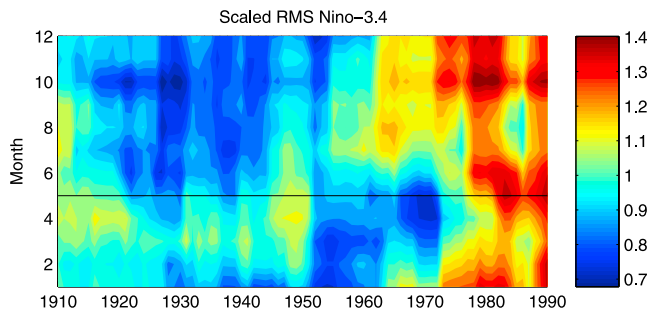

Figure 6. Relative change of standard deviation of Niño-3.4 for each month with time for a centered 21-year window.

with the previous December, and that the cold and warm phase Niñoo-3.4 magnitudes in May are comparable, due to the different seasonality of La Niña events. Furthermore, as a non-parametric method, rank correlation is robust against outliers. Rather, the reason for this relationship appearing in the period since the 1980s seems to be the increase in equatorial Pacific variability in spring.

[18] Seeking a physical pathway for the relationship, analysis of wind stress and sea surface height anomalies in the Atlantic supports the scenario proposed by *Latif and Barnett* [1995] in which ENSO induces zonal wind stress anomalies in the western equatorial Atlantic which, through equatorial wave dynamics, lead to SSTA anomalies in the central and eastern Atlantic. The correlation of wind stress with SSTA maximizes when wind leads by one month.

[19] The strong seasonality of ENSO influence on the Atlantic raises the question of where the seasonality arises. We initially hypothesized that the appearance of the Atlantic cold tongue in May was responsible, permitting strong reaction of the equatorial SST to WEA wind stress and possible coupled feedbacks. While the season of strong Atlantic cold tongue during May–August (Figure 2, crosses) may play some role, we find high correlation of Atl-3 SST to WEA wind stress during other seasons as well (Figure 2, squares). Instead, the correlation of Niño-3.4 to WEA stress, which is high from April to August (Figure 2, triangles), shows the strongest seasonal drop of the steps in the hypothesized path and most clearly reflects the seasonality of the Atl-3 to Niño-3.4 correlation. This places the cause for the seasonality on the atmospheric side.

[20] A comparison of Figures 1d and 5 reveals a difference in the spatial patterns of the influence of equatorial and northern tropical Atlantic SSTA, respectively, on South American rainfall in May. The precipitation anomalies concurrent with NTA SSTA are located over Brazil's Nordeste whereas equatorial SSTA are associated with rain anomalies in the northeastern Amazon and the Guiana Highlands.

[21] **Acknowledgments.** This work was supported under National Oceanic and Atmospheric Administration grants NA04OAR4310013 and NA05OAR4310007. This is IGPP contribution 6241.

References

Barreiro, M., and P. Chang (2002), Variability of the South Atlantic convergence zone simulated by an atmospheric general circulation model, *J. Clim.*, *15*, 746–763.

Carton, J. A., and B. Huang (1994), Warm events in the tropical Atlantic, *J. Phys. Oceanogr.*, *24*, 888–903.

Chang, P., L. Ji, and H. Li (1997), A decadal climate variation in the tropical Atlantic Ocean from thermodynamic air-sea interactions, *Nature*, *385*, 516–518.

Chang, P., R. Saravanan, L. Ji, and G. C. Hegerl (2000), The effect of local sea surface temperatures on atmospheric circulation over the tropical Atlantic sector, *J. Clim.*, *13*, 2195–2216.

Chiang, J. C. H., Y. Kushnir, and S. E. Zebiak (2000), Interdecadal changes in eastern Pacific ITCZ variability and its influence on the Atlantic ITCZ, *Geophys. Res. Lett.*, *27*, 3687–3690.

Chiang, J. C. H., Y. Kushnir, and A. Giannini (2002), Deconstructing Atlantic Intertropical Convergence Zone variability: Influence of the local cross-equatorial sea surface temperature gradient and remote forcing from the eastern equatorial Pacific, *J. Geophys. Res.*, *107*(D1), 4004, doi:10.1029/2000JD000307.

Delecluse, P., J. Servain, C. Levy, K. Arpe, and L. Bengtsson (1994), On the connection between the 1984 Atlantic warm event and the 1982–1983 ENSO, *Tellus, Ser. A*, *46*, 448–464.

Dommenget, D., and M. Latif (2000), Interannual to decadal variability in the tropical Atlantic, *J. Clim.*, *13*, 777–792.

Ducet, N., P. Y. L. Traon, and G. Reverdin (2000), Global high resolution mapping of ocean circulation from the combination of TOPEX/Poseidon and ERS-1/2, *J. Geophys. Res.*, *105*, 477–498.

Enfield, D. B., and E. J. Alfaro (1999), The dependence of Caribbean rainfall on the interaction of the tropical Atlantic and Pacific oceans, *J. Clim.*, *12*, 2093–2103.

Enfield, D. B., and D. A. Mayer (1997), Tropical Atlantic sea surface temperature variability and its relation to El Niño-Southern Oscillation, *J. Geophys. Res.*, *102*, 929–946.

Florenchie, P., J. R. E. Lutjeharms, C. J. C. Reason, S. Masson, and M. Rouault (2003), The source of Benguela Niños in the South Atlantic Ocean, *Geophys. Res. Lett.*, *30*(10), 1505, doi:10.1029/2003GL017172.

Giannini, A., J. C. H. Chiang, M. A. Cane, Y. Kushnir, and R. Seager (2001), The ENSO teleconnection to the Tropical Atlantic Ocean: Contribution of the remote and local SSTs to rainfall variability in the Tropical Americas, *J. Clim.*, *14*, 4530–4544.

Hastenrath, S., and L. Heller (1977), Dynamics of climatic hazards in northeast Brazil, *Q. J. R. Meteorol. Soc.*, *103*, 77–92.

Hettmansperger, T. P., and J. W. McKean (1998), *Robust Nonparametric Statistical Methods*, Edward Arnold, London.

Latif, M., and T. P. Barnett (1995), Interaction of the tropical oceans, *J. Clim.*, *8*, 952–964.

Merle, J. (1980), Variabilité thermique annuelle et interannuelle de l'Océan Atlantique équatorial est: L'hypothèse d'un El Niño Atlantique, *Oceanol. Acta*, *3*, 209–220.

Neelin, J. D., and H. Su (2005), Moist teleconnection mechanisms for the tropical South American and Atlantic sector, *J. Clim.*, *18*, 3928–3950.

Neelin, J. D., C. Chou, and H. Su (2003), Tropical drought regions in global warming and El Niño teleconnections, *Geophys. Res. Lett.*, *30*(24), 2275, doi:10.1029/2003GL018625.

Nobre, P., and J. Shukla (1996), Variations of sea surface temperature wind stress and rainfall over the tropical Atlantic and South America, *J. Clim.*, *9*, 2464–2479.

Reynolds, R. W., N. A. Rayner, T. M. Smith, D. C. Stokes, and W. Wang (2002), An improved in situ and satellite SST analysis for climate, *J. Clim.*, *15*, 1609–1625.

Ruiz-Barradas, A., J. A. Carton, and S. Nigam (2003), Role of the atmosphere in climate variability of the tropical Atlantic, *J. Clim.*, *16*, 2052–2065.

Saravanan, R., and P. Chang (2000), Interaction between tropical Atlantic variability and El Niño–Southern Oscillation, *J. Clim.*, *13*, 2177–2194.

Simmons, A. J., and J. K. Gibson (2000), The ERA-40 project plan, technical report, Eur. Cent. for Medium-Range Weather Forecasts, Reading, U.K.

Sutton, R. T., S. P. Jewson, and D. P. Rowell (2000), The elements of climate variability in the tropical Atlantic region, *J. Clim.*, *13*, 3261–3284.

Wang, C., S.-P. Xie, and J. A. Carton (2004), A global survey of ocean-atmosphere interaction and climate variability, in *Earth Climate: The Ocean-Atmosphere Interaction*, *Geophys. Monogr. Ser.*, vol. 147, edited by C. Wang, S.-P. Xie, and J. A. Carton, pp. 1–19, AGU, Washington, D. C.

Xie, P., and P. A. Arkin (1997), Global precipitation: A 17-year monthly analysis based on gauge observations satellite estimates and numerical model outputs, *Bull. Am. Meteorol. Soc.*, *78*, 2539–2558.

Zebiak, S. E. (1993), Air-sea interaction in the equatorial Atlantic region, *J. Clim.*, *6*, 1567–1586.

M. Münnich and J. D. Neelin, Department of Atmospheric and Oceanic Sciences, University of California, Los Angeles, CA 90095-1567, USA. (munnich@atmos.ucla.edu; neelin@atmos.ucla.edu)